Nuclear Engineering and Design 320 (2017) 65–76

Contents lists available at ScienceDirect

Nuclear Engineering and Design

journal homepage: www.elsevier.com/locate/nucengdes

Numerical investigation on the unsteady characteristics of reactor coolant pumps with non-uniform inflow

Long Yun, Wang Dezhong *, Yin Junlian, Hu Yaoyu, Ran Hongjuan

School of Mechanical Engineering, Shanghai Jiao Tong University, Shanghai 200240, China

HIGHLIGHTS

- The unsteady characteristics of the pumps with uniform and non-uniform inflow was researched.
- The difference of the performance and the pressure pulsation with different inflow are compared.
- Pressure pulsation signals are analysed using FFT, RMS and Peak-to-Peak Value method.
- The effect of non-uniform inflow on the radial force are analysed.

ARTICLE INFO

Article history:
Received 30 January 2016
Received in revised form 26 November 2016
Accepted 17 April 2017

Keywords:
Reactor coolant pumps
Pressure pulsation
Non-uniform inflow
Numerical prediction

ABSTRACT

The pumps are generally designed and are selected based on performance under uniform inflow with the straight pipe, but actually non-uniform suction flow occurs at the inlet of the reactor coolant pump due to the complex geometry in the channel head. It is sorely necessary to research the unsteady characteristics of the pumps with uniform and non-uniform inflow. In this paper, CFD approach is employed to analyse the inlet and outlet pressure pulsation characteristics of reactor coolant pumps with different inflows. The channel head induces non-uniform flow in the pump inlet, while straight pipe is with the uniform inlet flow. Meanwhile, the pressure pulsations at positions of the inlet and outlet with different inflows are investigated. And pressure pulsation signals are analysed using *FFT*, *RMS* and Peak-to-Peak Value methods. The differences of the pressure pulsation and its characteristic between the channel head and straight pipe at the inlet and outlet are obvious due to the different inflows of channel head and straight pipe. The pressure amplitudes of f_R, f_{RPF}, $2f_{RPF}$, $3f_{RPF}$, $4f_{RPF}$, $2f_{SPF}$ are analysed, and the predominant components of the inlet and outlet in pressure spectra locate at $2f_{RPF}$. Further, the non-uniform inflow leads to the offset of the X radial force and the Y radial force, which leads to the increasing of the asymmetric degrees of radial force. The non-uniform inflow increases the radial force at low frequency. In a word, it is expected that the present work provides a different view of designing pumps with the consideration of non-uniform inflow. It is very important to accurately evaluate the hydrodynamic characteristics with non-uniform inflow because of the safety of the nuclear reactor. In further study, experimental investigation on the pressure pulsations of the reactor coolant pump with channel head and straight pipe will be conducted and flow field of the inlet will be measured by PIV as well.

1. Introduction

The reactor coolant pump is one of the most important equipment in nuclear power plant. Reactor coolant pump is between the reactor and the steam generator, and is mainly used to force the coolant circulate in the primary circuit. Due to rotor–stator interaction, unsteady pressure pulsation has a direct impact on the stable and safe operation of pumps (Brennen). The pressure pulsations of the pump, as a boundary condition of reactor system, are usually the significant scientific issues.

In the advanced pressurized water reactor (APWR) reactor primary coolant system, two canned motor pumps are directly attached to the cold side of the steam generator (Sun et al., 2010), as shown in Fig. 1. The pumps are identical designs and are designed based on performance under uniform inflow with the straight pipe, but actually non-uniform suction flow is induced in the discharge pipe of the steam generator due to the complex geometry in the channel head, which might influence the

* Corresponding author.
E-mail addresses: longyunjs@sjtu.edu.cn (L. Yun), dzwang_sjtu@sina.com (W. Dezhong).

http://dx.doi.org/10.1016/j.nucengdes.2017.04.027
0029-5493/

Nomenclature

D_2	Impeller outlet diameter, 271.5 mm	f_R	Rotating frequency of impeller, 24.7 Hz
b_2	Impeller outlet width, 83 mm	f_{RPF}	Rotor passing frequency, 123.3 Hz
n_d	Rotating speed, 1480 r/min	f_{SPF}	Stator passing frequency, 271.3 Hz
ω	Angular velocity, 155 rad/s	u_2	Tangential velocity of impeller outlet, 21.03 m/s
η	Efficiency	Z_1	Impeller blade number, 5
D_1	Inlet pipe diameter, 300 mm	Z_2	Diffuser blade number, 11
p	Pressure, Pa	Φ_d	Nominal flow rate coefficient, $Q_d/(\omega D_2^2 b_2)$
C_p	Pressure coefficient, $p/(0.5\rho u_2^2)$	Ψ_d	Nominal head coefficient, $gH_d/(\omega^2 D_2^2)$
ρ	Water density, 1000 kg/m^3	n_s	Specific speed, $n_s = 3.65 n d Q_d^{0.5}/H_d^{0.75}$, 387.5

performance of the pumps (Cheng et al., 2014). Furthermore, an effective approach should be developed to research pressure pulsation of the pumps with uniform and non-uniform inflow, which is sorely necessitated.

Up to now, only few researchers have studied the effect of the non-uniform inflow on the performance of pumps. Van Esch (2009) investigated the performance of a mixed-flow pump and hydrodynamic forces on the impeller under non-uniform suction flow with experimental method, they found that the performance of the pump is influenced by the type of suction velocity profile and a considerable steady radial force appeared when the suction flow is non-uniform. Xu et al. (2005) used 2-D PIV method to study the flow patterns of non-uniform flows in a rectangular open suction passage. Huang et al. (2002) investigated the flow characteristics within connection between steam generator channel head and pump suction by experimental method and found that the axial vortex is eliminated and axial velocity is uniform in the outlet section of the nozzle of the channel head. But the interaction between the channel head and the pump has not been investigated since no pumps are connected to the channel head in the test loop. And then, Cheng et al. (2014) investigate the effect of the velocity distortion generated by the steam generator on the performance of the two pumps by CFD method, and the results suggest that the nozzle dam brackets should be installed in the outlet pipe of the steam generator.

Generally, unsteady pressure pulsation excites mechanical vibrations of the pump even at the design operating condition. Up to now, lots of investigations have been carried out to study the unsteady flow, and the fast Fourier transform (FFT) method has been proved to be the most effective tool to analyse pressure fluctuations characteristics. Yao et al. (2011) analysed both frequency domain and time-frequency domain in a double suction centrifugal pump based on FFT and time-frequency representation methods. Parrondo-Gayo et al. (2002) also investigated the unsteady pressure distribution in a conventional centrifugal pump, and they paid more attention on pressure pulsations at blade passage frequency. Some studies focus on the influence of geometry on pressure pulsation by either experimental or numerical method. Spence and Amaral-Teixeira (2009) explored the effects of pressure pulsation. In their work, they took the form of a parametric study covering four geometric parameters by numerical analysis. And a rationalisation process aimed at reducing vibration through reductions in pressure pulsations has produced geometric recommendations. Yang et al. (2012, 2014) investigated unsteady pressure fields of the pump as turbine by numerical methods and illustrated that increasing blade tip clearance serves as an effective measure for reducing pressure pulsation. Benra (2006) investigated the periodic unsteady flow in a single-blade pump by CFD simulation and particle image velocimetry measurement method, and the results show that transient numerical simulations compare very well to velocity measurements. Pei et al. (2012, 2013) conducted the numerical investigation on the periodically unsteady flow of a single-blade pump and predicted the flow in a whole passage.

Under off-design conditions, some unexpected flow phenomena superposed to the rotor-stator interaction have considerable effect on vibration and safety. Toussaint et al. (Toussaint, 2006) conducted experimental investigation on the unsteady flow in the pump in off-design conditions and concluded that the pressure fluctuations occur at blade passing frequency, rotation frequency, and their harmonics. Barrio et al. (2008, 2010) presented a study on the fluid-dynamic pulsations and the dynamic forces in a centrifugal pump with different radial gap between the impeller and the volute. They estimated the dynamic radial forces and torque at blade passing frequency, whereas the progressive reduction of

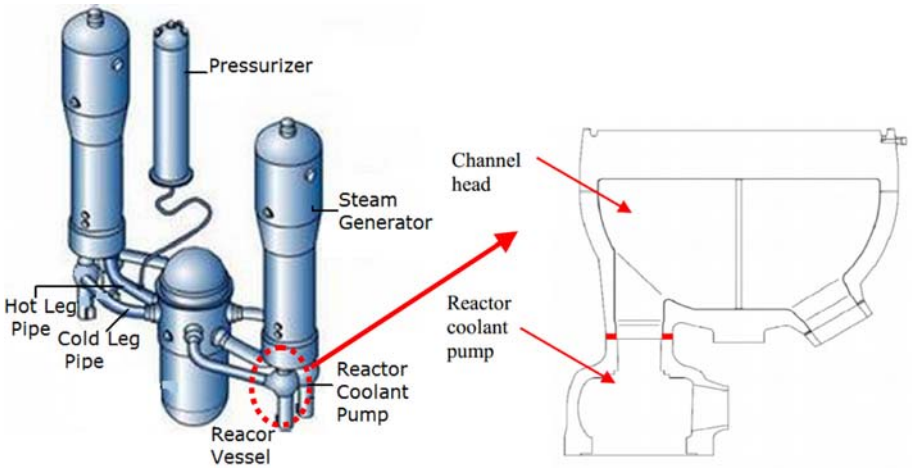

Fig. 1. Schematic diagram of connection type.

the impeller-tongue gap brought about corresponding increments in dynamic load. Wang and Tsukamoto (2003) investigated the unsteady phenomena in a diffuser pump at the off-design conditions by a two-dimensional vortex method. The results showed an asymmetrical separation bubble causes the unsteady flow near the pressure surface of the impeller vane. Zhang et al. (2015) explored a slope volute pump to reduce the level of pressure pulsation, and used numerical simulation to analyse its influence on flow structures.

These researchers have done a lot of work on the pressure pulsation of the pump with straight pipe inflow. However, these researches did not consider the effect of non-uniform inflow on the pressure pulsations due to the complex geometry in the channel head. The pressure pulsations at the inlet and outlet are significant input condition for the design of the nuclear reactor. It is sorely necessary to research the pressure pulsation of the pumps with uniform and non-uniform inflow.

Therefore, in this paper, CFD approach was employed to analyse pressure pulsation characteristics of a scaled model reactor coolant pump with different inflows. The three-dimensional pump internal flow channel was modelled by pro/E software, Reynolds-averaged Naiver-Stokes equations with the k-ε turbulence model were solved by the computational fluid dynamics software CFX to conduct the steady and unsteady numerical simulation, by which the flow field and pressure pulsations were obtained. Detailed analysis of pressure spectrum is performed by Fast Fourier Transform (FFT) method, and special attention is paid to compare pressure pulsation peaks at blade passing frequency with different inflows.

2. Experiment

2.1. The test rig

A test rig was developed in order to investigate the pump hydrodynamics and the pressure pulsations, in Fig. 2. It consists of a set of pipes and vanes, which form an open hydraulic circuit, and a reactor coolant model pump actuated by a 55 kW asynchronous motor. Diameters of inlet and outlet pipes are 0.30 m and 0.25 m, respectively.

Two pressure transducers is installed on the rig to acquire pressure at the inlet and outlet sections of the pump, as shown in Fig. 2. In order to measure the discharge, an electromagnetic flow meter is installed on the rig. The range of flow meter is 0–1500 m^3/h with an accuracy reported to be ±0.5%.

3. Numerical simulation

3.1. Pump model

The hydraulic components of the pump mainly consist of mixed flow impeller, twisted radial diffuser and pump casing. The pump casing is made to be spherical shaped considering high operating pressure and strength of the pump structure. The geometry models of the impeller, diffuser and pump casing are created by 3D modeling software Pro/E. Fig. 1 shows the cold side of the steam generator with two discharging pipes. Since the cold side of the steam generator is symmetric, it is assumed that the flow field inside is also symmetrical. So the channel head could be divided into two mirror parts. The effect of the channel head and straight pipe on the performance of the pump can be investigated individually. The two model pumps are identical designs, and the parameters of the pump are shown in Table 1. The nominal flow rate $Q_d = 950\ m^3/h$ and the nominal head of the model pump $H_d = 13.5$ m. The computational domain includes the channel head, straight pipe, impeller, diffuser, spherical casing with straight outlet pipe, as shown in Fig. 3.

3.2. Monitor points

In order to monitor the unsteady pressure pulsation in the inlet and outlet of the model pump, the points of I_1–I_8 are set at the inlet section apart from the impeller at a distance of D_1, and the points of O_1–O_8 are set at the outlet section apart from the impeller at a distance of D_1, as shown in Fig. 3(c).

3.3. Mesh

In order to improve the grid quality, nearly all the computational domains are meshed by the hexahedral elements, except for the channel head with complex geometry. The grid independence test has been done in our previous work (Yun et al., 2016). The grids of the impeller, diffuser and casing are shown in Fig. 4. The magnitude of y+ around the blades is lower than 200. Grid number of each domain is shown in Table 1.

3.4. Boundary condition and solution method

A steady calculation with frozen rotor strategy was done in advance to provide a starting solution. The working medium is water at 25 °C. The rotation of the impeller is set to be 1480 r/min. The mass flow rate at inlet and the pressure at outlet are set as the boundary condition. The adiabatic and no-slip boundary condition is applied to the solid walls. The k-ε turbulent model is chosen to solve the RANS equation. The interface between the impeller and the diffuser is set to 'transient rotor-stator', the interface between the impeller and the suction pipe is also set to 'transient rotor-stator'. The time step Δt is 3.3784×10^{-4} s, corresponding to the changed angle of 3° of impeller rotation. Ten revolutions of the impeller for the design condition are conducted. The upwind scheme is chosen for advection terms and the transient scheme is second order backward Euler. Initially, the transient timestep is set to be 'Automatic', which is a functionality provided by CFX software. Within each time step, the number of iterations has been chosen to 25. The residual convergence precision of the steady calculation is set to 10^{-4}.

4. Results and discussions

4.1. Hydraulic performance

Fig. 5 shows the pump hydraulic performance of different suction flows and the experiment, and the experiment is conducted with the straight pipe. The numerical results of the straight pipe and channel head were validated with experimental data for the heads at different flow coefficients. In the nominal flow rate, it can be seen that the head of the pump with the channel head decreases by 3.51% when compared to the experiment, the head of the pump with the straight pipe decreases by 2.35% when compared to the experiment, the head of the pump with the channel head decreases by 1.19% when compared to the straight pipe. It can be concluded that the suction flow coming from the channel head of the steam generator has a considerable effect on the performance of the canned motor pumps.

4.2. Flow field analysis

To clarify the reason leading to the difference of pump performance with different inflows, Fig. 6 presents static pressures at the inlet and outlet. In Fig. 6(a), at nominal flow rate, the pressure

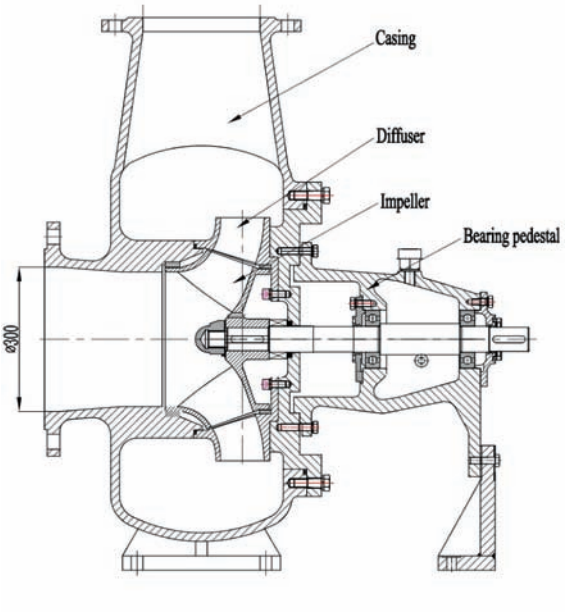

(a) The model pump

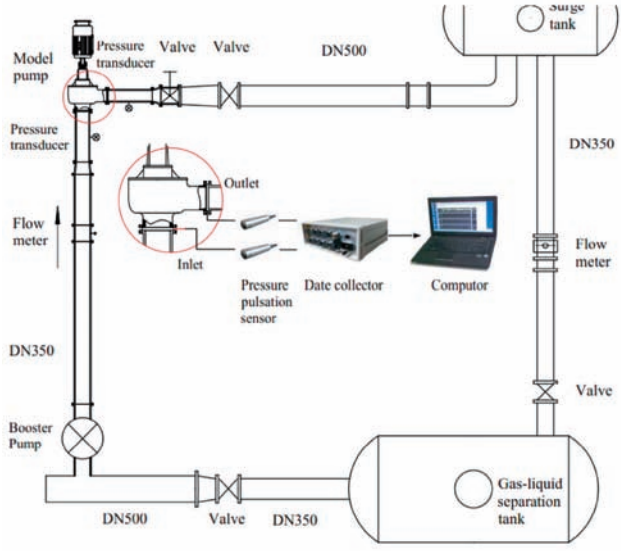

(b) Schematic diagram

(c) The test rig

Fig. 2. Overview of the test rig and the model pump.

Table 1
Grid number of domains.

Domain	Straight inlet pipe		Channel head
Grid number	1,214,400		1,967,476,
Domain	Impeller	Diffuser	Casing
Grid number	1,132,405	1,919,775	1,276,405

at the inlet with the straight pipe is well symmetrical, the pressure increases annularly from the center to the pipe wall. In Fig. 6(b), the pressure at the inlet with the channel head is asymmetry, and the low pressure region is at the upper left. It indicates that the channel head leads to non-uniformity of the pressure distribution at the inlet. In Fig. 6(c) and (d), the low pressure region at the outlet with the straight pipe is obviously different from the channel head, and the pressure field structure at the outlet with the straight pipe is entirely different from the channel head.

Fig. 7 presents the velocity at the outlet with different suction flows. Compared with Fig. 7(a) and (b), the low velocity region with the straight pipe is mainly at the top, and the low velocity region with the channel head is mainly at the right. Fig. 8 shows

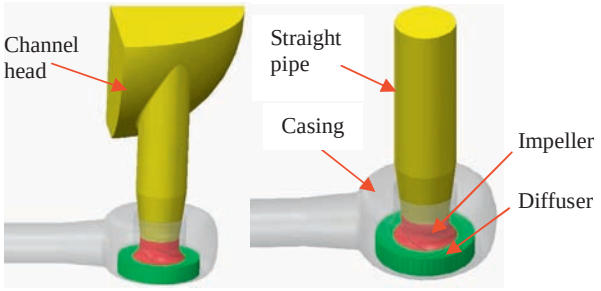

(a) The model with channel head (b) The model with straight pipe

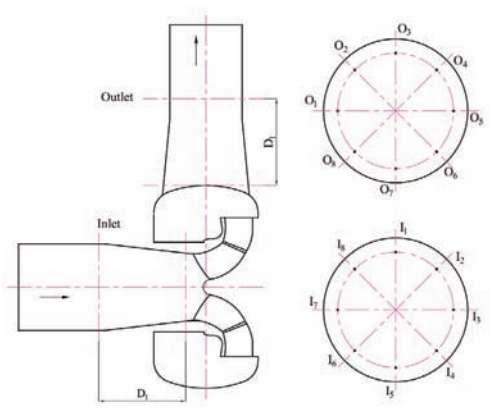

(c) The monitor points

Fig. 3. The computational domains and monitor points.

Fig. 4. The grids of each component.

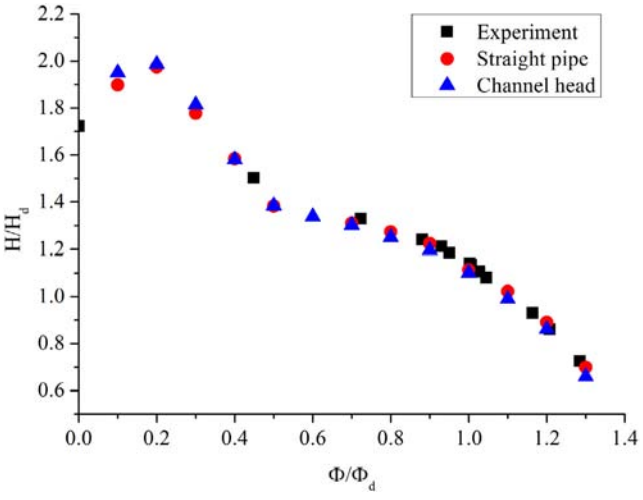

Fig. 5. The performance of the pump compared with CFD and experiment.

the velocity arrow at the inlet region apart from the impeller at a distance of D_1 with different suction flows. In Fig. 8(a), the velocity with channel head is non-uniform, similar to the flow in an elbow pipe where secondary flow is induced by the centrifugal force.

It is evident that the two different inflows of channel head and straight pipe induce the difference of inlet flow, the channel head induces the inlet flow non-uniform, and the non-uniformity of the inflow induces the outlet flow with channel head different from that with the straight pipe. The reason for the variation of pump performance is probably related to inflows structures with the channel head and straight pipe.

4.3. Unsteady pressure pulsation at the inlet and outlet of the model pump

To evaluate pressure pulsation energy in particular frequency band, Root Mean Square (*RMS*) method and Peak-to-Peak Value (*VPP*) method were applied to deal with discrete pressure signals, as presented in Eqs. (1)–(5),

$$RMS = \frac{1}{0.5\rho u_2^2}\sqrt{\frac{1}{n}\sum_{i=1}^{n}(A_i - \bar{A})^2} \tag{1}$$

$$\bar{A} = \frac{1}{0.5\rho u_2^2}\frac{1}{n}\sum_{i=1}^{n}A_i \tag{2}$$

where A_i represents pressure amplitudes at different frequencies, and $\bar{A}$ is the mean amplitude.

$$VPP = Y_{max} - Y_{min} \tag{3}$$

$$Y_{max} = \frac{1}{0.5\rho u_2^2}MAX(A_1, A_2, \ldots, A_n) \tag{4}$$

$$Y_{min} = \frac{1}{0.5\rho u_2^2}Min(A_1, A_2, \ldots, A_n) \tag{5}$$

where Y_{max} represents the maximum value of all datum, Y_{min} represents the minimum value of all datum.

In the centrifugal pump, the small gap between the rotating impeller and the stationary vane leads to intense pressure fluctuation (Choi et al., 2003; Gao et al., 2014). Unsteady pressure pulsation simulations of the model pump were conducted at the inlet and outlet in the design flow rates. Fig. 9 shows unsteady pressure pulsation of the inlet monitor points with different suction flows in the nominal flow rate. T means a cycle. In Fig. 9 and following figures, 1.0T in the horizontal axis indicates a full cycle of the impeller. As observed, the pressure signals fluctuate obviously. As shown in Fig. 9(a), the pressure pulsations of I_1–I_8 have little difference, which is associated with the uniform inflow when the inlet is the straight pipe. Fig. 9(b) shows the pressure pulsations of the inlet with channel head, there are some differences between the I_1–I_8, which is associated with the non-uniform flow structure in the channel head and inlet pipe. According to Figs. 6–8, the non-uniform phenomenon occurs within the channels head and inlet pipe.

Fig. 10 shows unsteady pressure pulsation of the outlet monitor points with different suction flows in the nominal flow rate. As observed, the pressure signals fluctuate obviously. The non-uniform suction flow, of course, influences the overall hydrodynamic performance of the model pump and induces rather high amplitude pressure pulsation. The differences of the pressure pulsation between the channel head and the straight pipe is need further study.

Fig. 11 shows unsteady pressure pulsation of the outlet monitor point O_1 with different suction flows of the channel head and

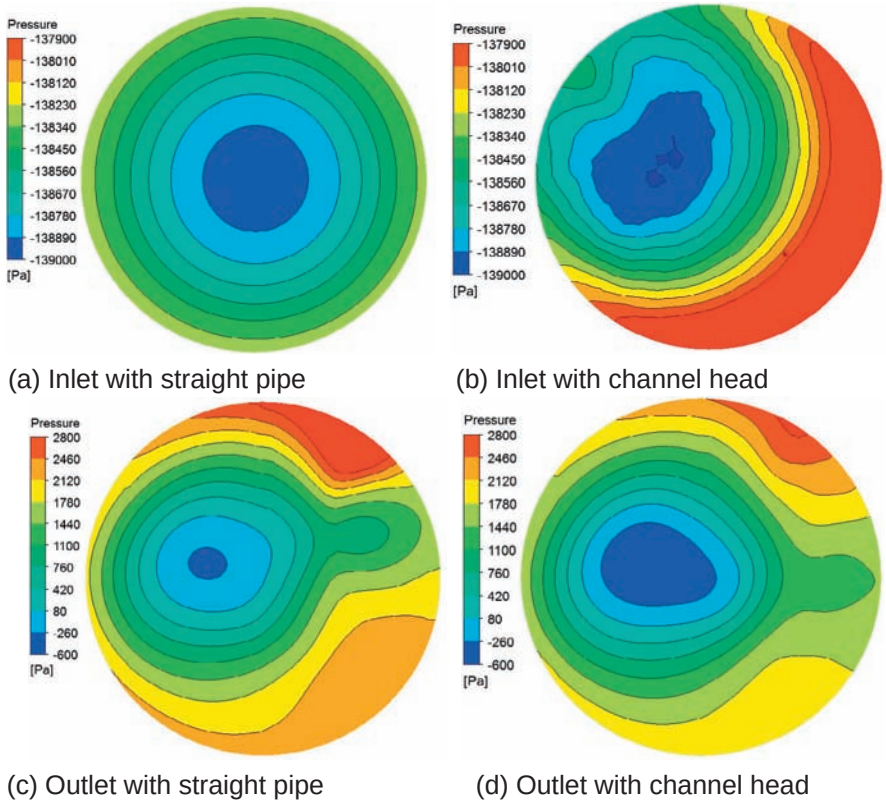

Fig. 6. The pressure at the inlet and outlet with different suction flows.

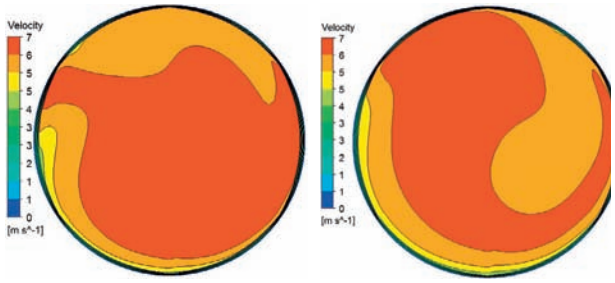

Fig. 7. The velocity at the outlet with different suction flows.

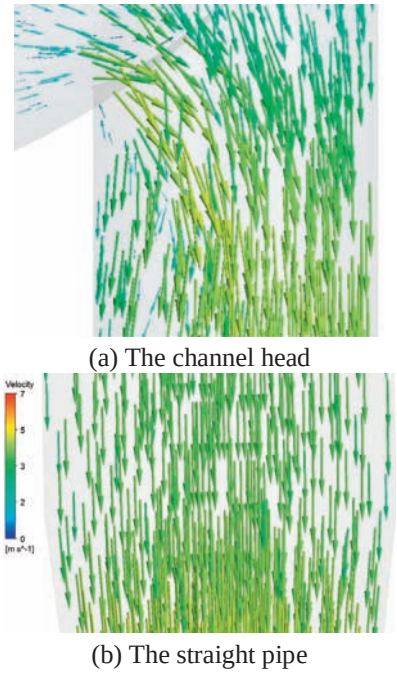

Fig. 8. The velocity at the inlet with different suction flows.

straight pipe. From O_1 to O_8, we choose O1 as an example. It can be found that the differences of the pressure pulsation between the channel head and straight pipe are obviously. It is evident that the two different inflows of channel head and straight pipe have significant effect on the pump unsteady pressure pulsation.

4.4. The characteristic value of pressure pulsation at the inlet and outlet of the model pump

The characteristic values of pressure pulsation at the inlet monitor points with the channel head and straight pipe are shown in Fig. 12. As illustrated in Fig. 12(a), the *VPP* at I_1–I_8 with the channel head hardly changes, the *VPP* at I_1–I_8 with the straight pipe also changes very little, and the *VPP* of the channel head is almost 4.42% lower than the straight pipe. In Fig. 12(b), the *RMS* with the channel head has the largest value at I_7 point and the smallest value in I_4 point, the *RMS* at I_1–I_8 with the straight pipe changes very little, and it is the largest difference that the *RMS* of the channel head is 0.730% higher than the straight pipe and the smallest difference that the *RMS* of the channel head is 0.034% higher than the straight pipe.

The characteristic values of pressure pulsation at the outlet monitor points with the channel head and straight pipe are shown in Fig. 13. As illustrated in Fig. 13(a), the *VPP* with the channel head

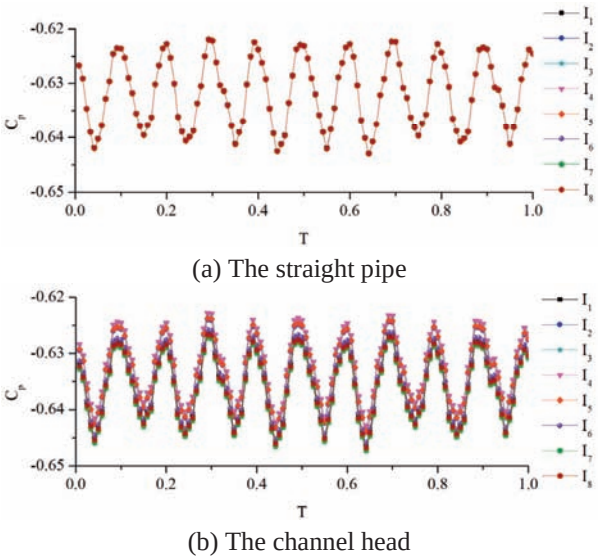

(a) The straight pipe

(b) The channel head

Fig. 9. The pressure pulsation of the inlet with different suction flows.

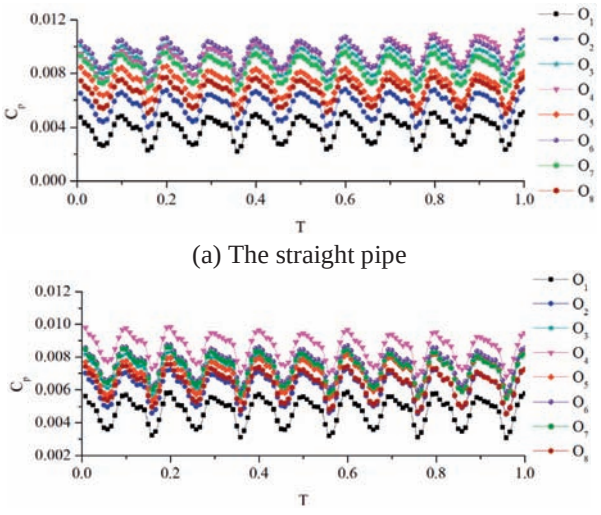

(a) The straight pipe

(b) The channel head

Fig. 10. The pressure pulsation of the outlet with different suction flows.

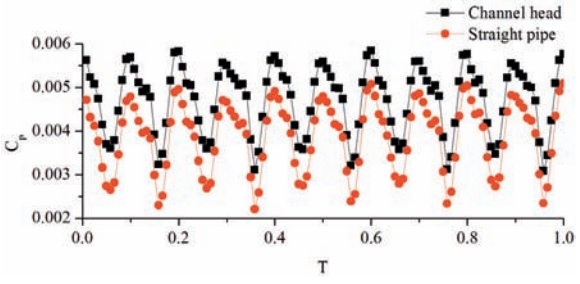

Fig. 11. The pressure pulsation of different inflows at O_1.

has the largest value at O_7 point and the least value at O_1 point, the *VPP* with the channel head changes a little, the *VPP* with the straight pipe has the largest value at O_4 point and the least value at O_6 point, and it is the largest difference at O_4 point that

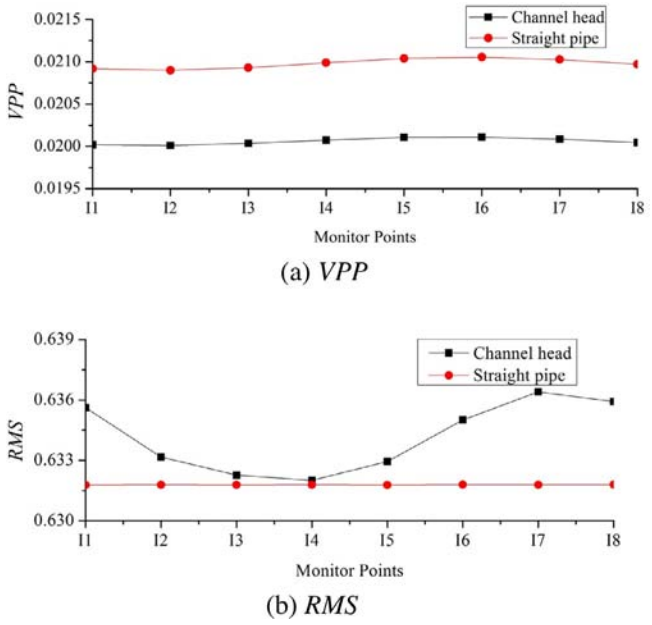

Fig. 12. The characteristic value of pressure pulsation with different suction flows at inlet.

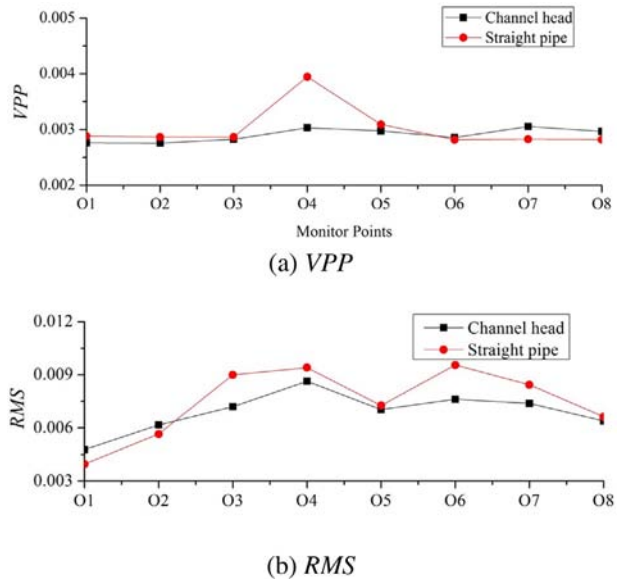

Fig. 13. The characteristic value of pressure pulsation with different suction flows at outlet.

the *VPP* of the channel head is 14.289% lower than the straight pipe and the smallest difference at O_5 point that the *VPP* of the channel head is 0.307% lower than the straight pipe. In Fig. 13(b), the *RMS* with the channel head has the largest value at O_4 points and the least value in O_1 points, the *RMS* with the straight pipe has the largest value at O_6 point and the smallest value at O_1 point, and it is the largest difference at O_1 point that the *RMS* of the channel head is 20.751% higher than the straight pipe and the least difference at O_5 point that the *RMS* of the channel head is 3.197% lower than the straight pipe.

At the points of the inlet and outlet, the differences of the pressure pulsation characteristic value between the channel head and straight pipe are obviously.

4.5. The pressure spectra of pressure pulsation at the inlet and outlet of the model pump

To investigate the influence of the position on pressure pulsation characteristics, pressure spectra at I_1–I_8 of the inlet and O_1–O_8 of the outlet with different suction flows are presented in Figs. 14 and 15. In the centrifugal pump, rotor-stator interaction is a primary reason for high amplitude pressure pulsation. The rotating frequency of impeller f_R, rotor passing frequency f_{RPF}, stator passing frequency f_{SPF}, and their higher harmonics $2f_{RPF}$, $3f_{RPF}$, $4f_{RPF}$, $2f_{SPF}$ *etc.* are expected thereby. From Fig. 14, it is easy to identify f_{RPF} and its higher harmonics at different inlet points. The predominant components in pressure spectra locate at $2f_{RPF}$, and the corresponding amplitudes are larger than other harmonics. Some prominent discrete components at f_{RPF}, $3f_{RPF}$, $2f_{SPF}$ can be identified for I_1–I_8. The peak distribution of the straight pipe is similar to that of the channel head. From Fig. 15, it is easy to identify f_{RPF} and its higher harmonics at different outlet points. The predominant components in pressure spectra locate at $2f_{RPF}$, and the corresponding amplitudes are larger than other harmonics. Some prominent discrete components at f_{RPF}, $3f_{RPF}$, $4f_{RPF}$ can be identified for I_1–I_8. The peak distribution of the straight pipe is similar to that of the channel head.

Fig. 16 shows the pressure amplitudes at distinct peaks of the inlet points I_1–I_8 with different suction flows. As illustrated in Fig. 16(a), the pressure amplitudes at f_{RPF} of the channel head and straight pipe all change very little at the inlet points I_1–I_8, the pressure amplitudes at f_{RPF} of the channel head are almost 57.5% higher than that of the straight pipe. In Fig. 16(b)–(d), the pressure amplitudes at $2f_{RPF}$, $3f_{RPF}$ and $2f_{SPF}$ of the channel head and straight pipe all change very little at the inlet points I_1–I_8. The pressure amplitudes at $2f_{RPF}$ of the channel head are almost 12.15% lower than that of the straight pipe. The reason may be that the non-uniform inflow lower the $2f_{RPF}$ intensity. The pressure amplitudes at $3f_{RPF}$ of the channel head are almost 13.1% higher than that of the straight pipe. The pressure amplitudes at $2f_{SPF}$ of the channel head are almost 3.0% higher than that of the straight pipe.

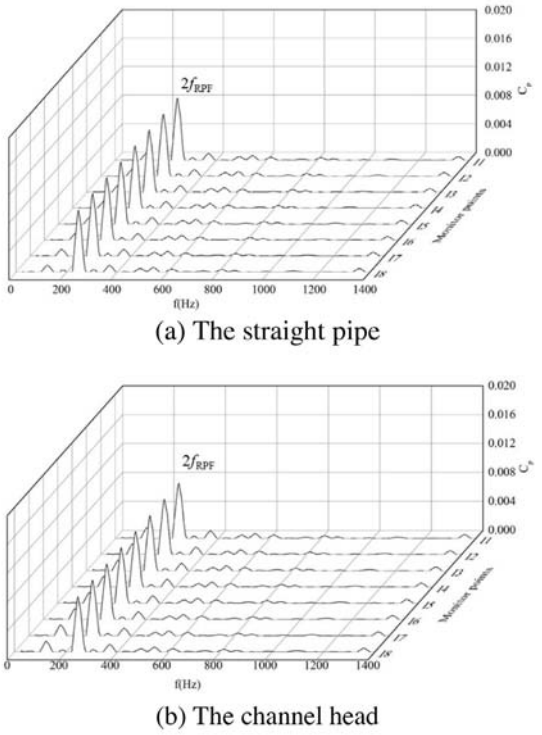

Fig. 14. The frequency domain of the inlet with different suction flows.

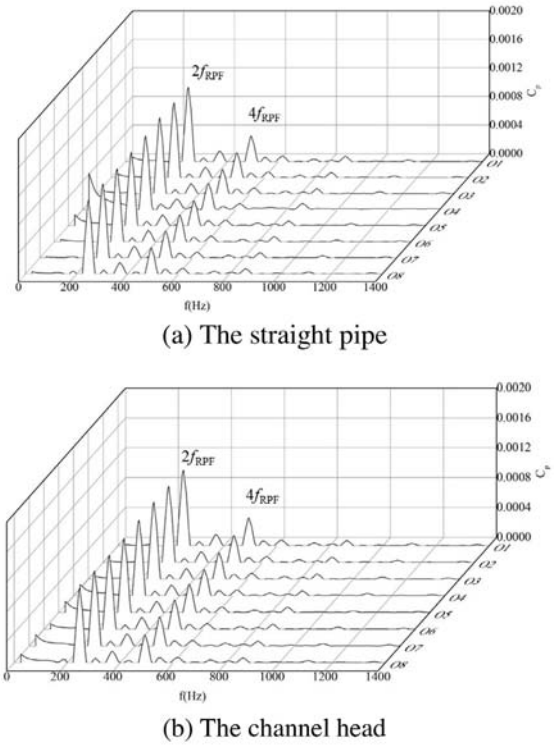

Fig. 15. The frequency domain of the outlet with different suction flows.

Fig. 17 shows the pressure amplitudes at distinct peaks of the outlet points O_1–O_8 with different suction flows. As illustrated in Fig. 17(a), the pressure amplitude at f_R with the channel head has the largest value at O_4 and O_7 points and the least value in O_1 point, the pressure amplitude at f_R with the straight pipe has the largest value at O_4 point and the least value at O_7 point. The maximal difference of the pressure amplitude at f_R between the channel head and straight pipe is at O_4. From Fig. 6, we can find O_4 point is at the position where the pressures are maximum. And in this region the pressure distribution and the pressure amplitude at the dominant frequency and its harmonics are more affected.

In Fig. 17(b), the variation trend of the pressure amplitude at $2f_{RPF}$ with the channel head is similar to straight pipe, and the pressure amplitude at $2f_{RPF}$ of the channel head is 1.92%–3.36% lower than that of straight pipe. In Fig. 17(c), the variation trend of the pressure amplitude at $3f_{RPF}$ with the channel head is almost similar to straight pipe, and the difference between the channel head and straight pipe is very little except for O_4 point, where the pressure amplitude of the channel head is 5.66% lower than the straight pipe. In Fig. 17(d), the variation trend of the pressure amplitude at $4f_{RPF}$ with the channel head is almost similar to straight pipe except for O_4 point, where the pressure amplitude of the channel head is 4.94% lower than the straight pipe, while in other points the pressure amplitude of the channel head is 2.95%–8.68% higher than the straight pipe.

4.6. Discussion

The flow and the pressure pulsation of the reactor coolant pumps with uniform and non-uniform inflow were researched.

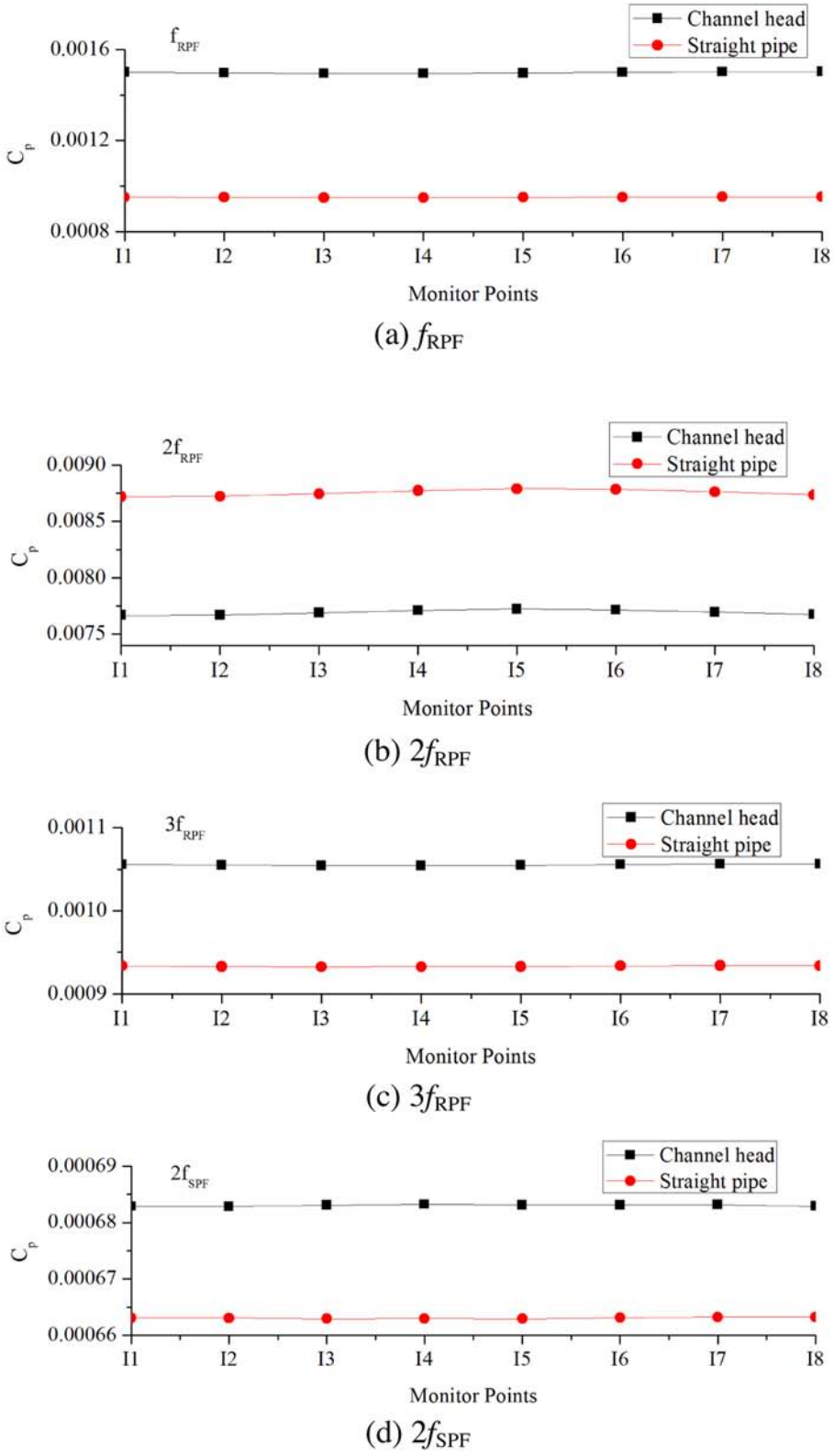

Fig. 16. Pressure amplitudes at distinct peaks of the inlet with different suction flows.

From the above results and analysis, we can find that two different inflows of channel head and straight pipe induce the difference of inlet flow, the channel head induces the inlet flow non-uniform. And two different inflows induce the differences of the pressure pulsation characteristic value between the channel head and straight pipe. Fig. 18 shows the velocity between blades at middle span of the impeller with different suction flows. It can been seen that the velocity distribution in the non-uniform suction condition

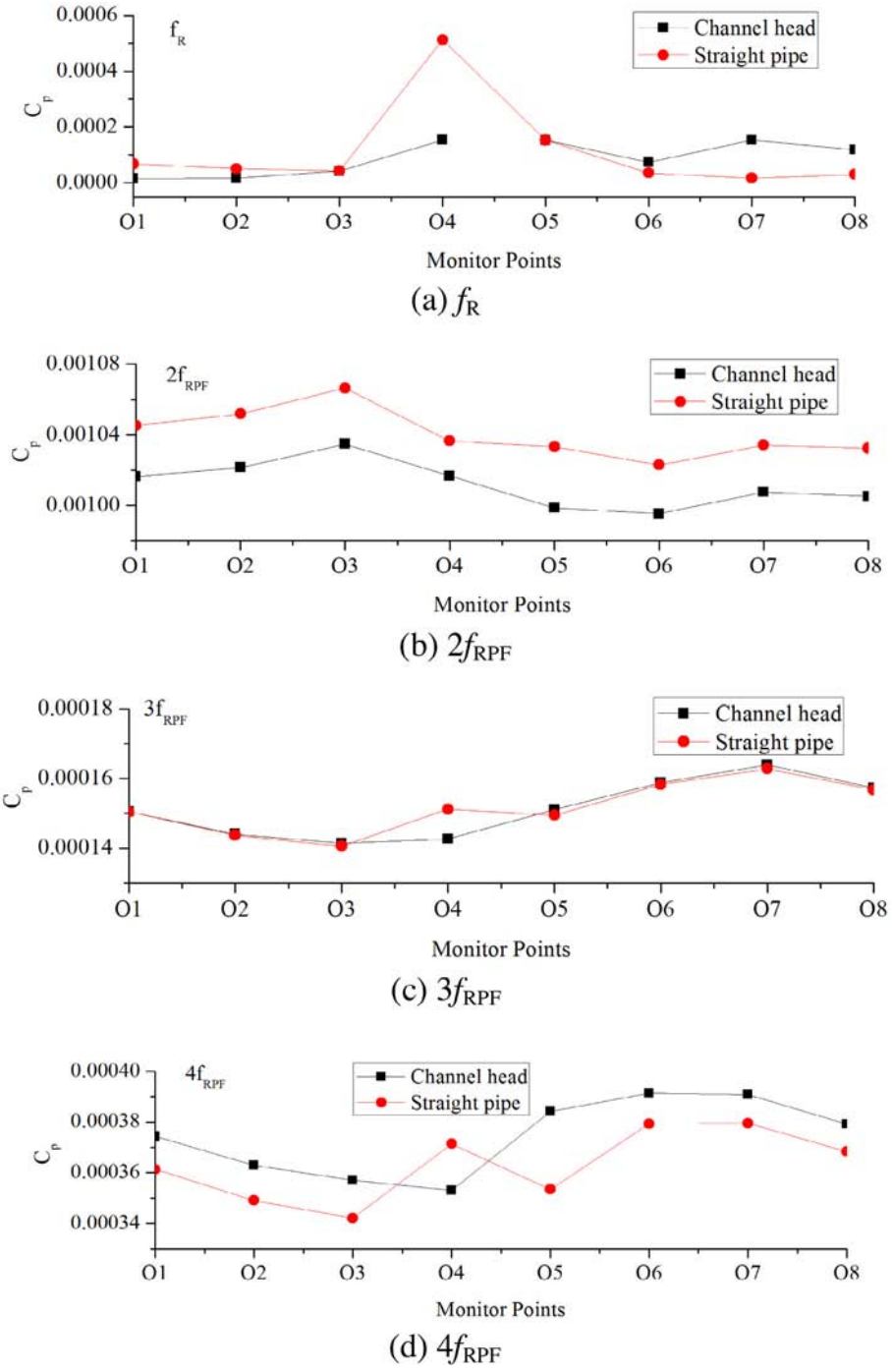

Fig. 17. Pressure amplitudes at distinct peaks of the outlet with different suction flows.

is obviously different from that in the uniform suction flow. More specifically, the non-uniform suction flow lead to the velocity between blades non-uniform. While the incidence angle will increase when axial velocity and tangential velocity are non-uniform, which will cause the increase of impact loss and mixing loss [3]. This is the reason that leads to the difference of the pump performance and unsteady pressure pulsation between the channel head and straight pipe.

Meanwhile, the non-uniform inflow also leads to the differences of radial force. Fig. 19 shows the X radial force and the Y radial force of the impeller with different suction flows. From Fig. 19 (a) and (b), when the pump is connected with channel head, the non-uniform inflow leads to the offset of the X radial force and the Y radial force, and this offset leads to the asymmetric degrees of radial force increase. It will increase the risk of rotor-bearing system. Fig. 20 shows the radial force frequency domain of the impeller with different suction flows. From Fig. 20, the predominant components in force spectra locate at f_{SPF}, where the corresponding amplitudes of straight pipe and channel head are almost same. But at the frequency f_R, the corresponding amplitude of channel head are more than twice as much as the straight pipe. That means the non-uniform inflow increases the radial force at low frequency, which may leads to the low-frequency vibration of the shaft system.

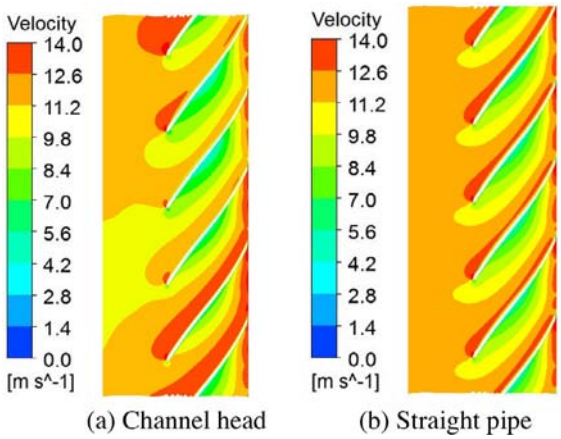

Fig. 18. The velocity between blades of the impeller with different suction flows.

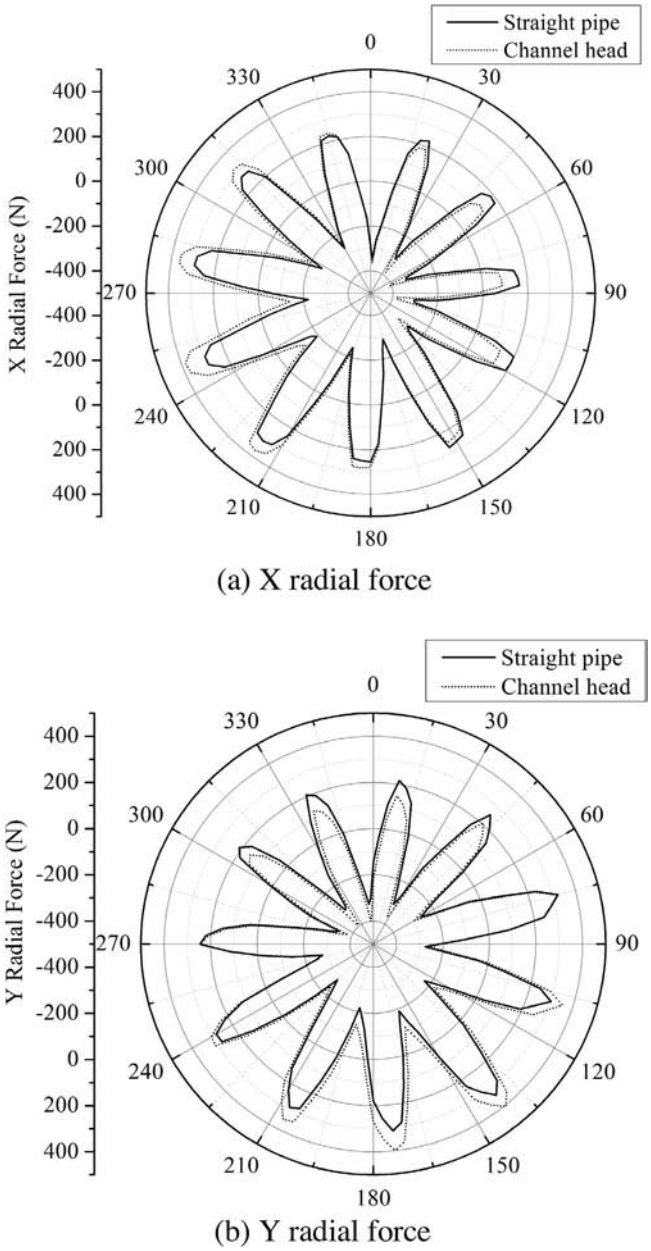

Fig. 19. The radial force of the impeller with different suction flows.

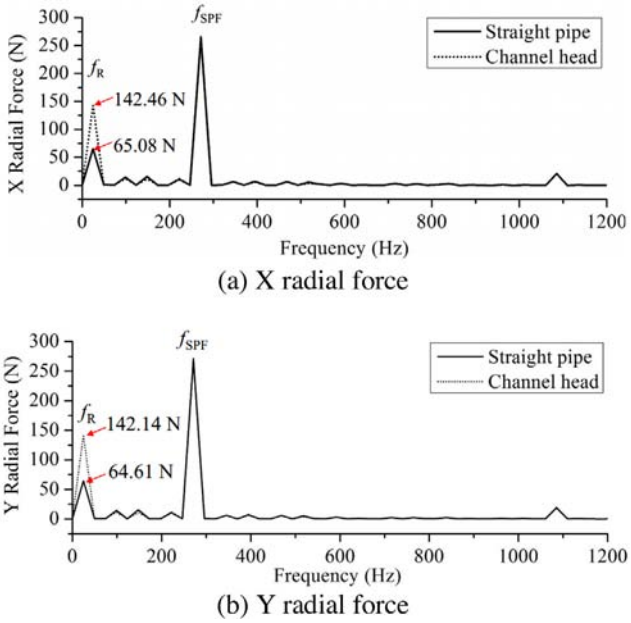

Fig. 20. The radial force frequency domain of the impeller with different suction flows.

5. Conclusion

Numerical investigation on unsteady pressure pulsation features of a scaled model reactor coolant pump with different inflows are presented. The pump hydraulic performance with the straight pipe is measured by experimental method, and the head is compared to that of the channel head and the straight pipe obtained by numerical method. The flow fields at the inlet and outlet of different inflows are obtained. The analysis focuses on pressure pulsations at positions of the inlet and outlet in the nominal flow rate. Pressure pulsation signals are analysed using *FFT*, *RMS* and Peak-to-Peak Value methods.

The numerical results of the straight pipe and channel head were validated with experimental data for the heads at different flow coefficients. In the nominal flow rate, the head of the pump with the channel head decreases by 1.19% when compared to the straight pipe. It can be concluded that the suction flow coming from the channel head of the steam generator has a considerable effect on the performance of the canned motor pumps.

From the flow fields of the inlet and outlet, it is evident that the two different inflows of channel head and straight pipe induce the difference of inlet flow, the channel head induces the inlet flow non-uniform, and the non-uniformity of the inflow induces the outlet flow with channel head different from the straight pipe. The reason for the change of pump performance is probably related to inflow structures with the channel head and straight pipe.

Meanwhile, the pressure pulsations of different inflows are investigated. The global instability inflow induces rather high amplitude pressure pulsation. The differences of the pressure pulsation between the channel head and straight pipe at the inlet and outlet are obviously. At the points of the inlet and outlet, the pressure pulsation characteristics between the channel head and straight pipe are compared, and the difference is obvious. It is evident that the two different inflows of channel head and straight pipe have significant effects on the pump unsteady pressure pulsation.

To assess the pressure amplitudes at distinct peaks at the points of the inlet and outlet with different suction flows, the pressure amplitudes at f_R, f_{RPF}, $2f_{RPF}$, $3f_{RPF}$, $4f_{RPF}$, $2f_{SPF}$ are analysed for com-

parison. The predominant components of the inlet and outlet in pressure spectra both locate at $2f_{RPF}$.

The non-uniform inflow also has effect in the radial force. The non-uniform inflow leads to the offset of the X radial force and the Y radial force, and this offset leads to the asymmetric degrees of radial force increase. And at the frequency f_R, the corresponding amplitude of channel head are more than twice as much as the straight pipe.

Finally, it is expected that the present work will provide a different view considering non-uniform inflow in design of the pump, which is different from the conventional design. The effects of non-uniform inflow on the pump performance and unsteady pressure pulsation are absolutely different from the uniform inflow. It is very important to accurately evaluate the performance with non-uniform inflow because it is directly related to the design and safety of the nuclear reactor. In further study, experimental investigation on the pressure pulsations of the reactor coolant pump with channel head and straight pipe will be conducted and flow field of the inlet will be measured by PIV as well.

Acknowledgments

This work is funded by 'Shanghai Economy Information Technology Committee' – 'China' and 'National Natural Science Foundation of China' – 'China' (No. 51576125).

References

Barrio, R., Blanco, E., Parrondo, J., GonzÃĄlez, J., FernÃĄndez, J., 2008. The effect of impeller cutback on the fluid-dynamic pulsations and load at the blade-passing frequency in a centrifugal pump. ASME J. Fluids Eng. 130, 111102.

Barrio, R., Parrondo, J., Blanco, E., 2010. Numerical analysis of the unsteady flow in the near-tongue region in a volute-type centrifugal pump for different operating points. Comput. Fluids 39, 859–870.

Benra, F.-K., 2006. Numerical and experimental investigation on the flow induced oscillations of a single-blade pump impeller. ASME J. Fluids Eng. 128, 783–793.

Brennen, C.E., 1994. Hydrodynamics of Pumps. Concepts ETI Inc., Oxford Science Publications, p. 81.

Cheng, H., Li, H., Yin, J., Gu, X., Hu, Y., Wang, D., 2014. Investigation of the distortion suction flow on the performance of the canned nuclear coolant pump. In: Conference: ISFMFE2014, At Wuhan, China.

Choi, J.-S., McLaughlin, D.K., Thompson, D.E., 2003. Experiments on the unsteady flow field and noise generation in a centrifugal pump impeller. J. Sound Vib. 263, 493–514.

Gao, Z., Zhu, W., Lu, L., Deng, J., Zhang, J., Wuang, F., 2014. Numerical and experimental study of unsteady flow in a large centrifugal pump with stay vanes. ASME J. Fluids Eng. 136, 071101.

Huang, W., Zhang, W.-Q., Tao, W.-Q., He, J.-S., Huang, H., Zhang, F.-Y., Liu, X.-B., 2002. Flow characteristics experimental study within connection between steam generator channel head and pump suction. Nucl. Power Eng. 23, 38–42.

Parrondo-Gayo, J.L., Gonzalez-Perez, J., Fernández-Francos, J.n., 2002. The effect of the operating point on the pressure fluctuations at the blade passage frequency in the volute of a centrifugal pump. ASME J. Fluids Eng. 124, 784–790.

Pei, J., Yuan, S., Benra, F.-K., Dohmen, H.J., 2012. Numerical prediction of unsteady pressure field within the whole flow passage of a radial single-blade pump. ASME J. Fluids Eng. 134, 101103.

Pei, J., Yuan, S., Yuan, J., 2013. Numerical analysis of periodic flow unsteadiness in a single-blade centrifugal pump. Sci. China Technol. Sci. 56, 212–221.

Spence, R., Amaral-Teixeira, J., 2009. A CFD parametric study of geometrical variations on the pressure pulsations and performance characteristics of a centrifugal pump. Comput. Fluids 38, 1243–1257.

Sun, H.-h., Cheng, P.-d., Miao, H.-x., 2010. The Third Generation of Nuclear Power Technology AP1000. China Electric Power Press, Beijing.

Toussaint, M., 2006. Analysis of unsteady flow in centrifugal pump at off-design point operation. In: Proceeding of 23rd IAHR Symposium on Hydraulic Machinery and Systems, Yokohama, Japan, Paper.

Van Esch, B., 2009. Performance and radial loading of a mixed-flow pump under non-uniform suction flow. ASME J. Fluids Eng. 131, 051101.

Wang, H., Tsukamoto, H., 2003. Experimental and numerical study of unsteady flow in a diffuser pump at off-design conditions. ASME J. Fluids Eng. 125, 767–778.

Xu, Z., Yi, F., Liu, S., Wu, Y., 2005. 2D PIV experiments on non-uniform flow in a rectangular open model pump suction passage. In: ASME 2005 International Mechanical Engineering Congress and Exposition. American Society of Mechanical Engineers, pp. 523–530.

Yang, S.-S., Kong, F.-Y., Chen, H., Su, X.-H., 2012. Effects of blade wrap angle influencing a pump as turbine. ASME J. Fluids Eng. 134, 061102.

Yang, S.-S., Liu, H.-L., Kong, F.-Y., Xia, B., Tan, L.-W., 2014. Effects of the radial gap between impeller tips and volute tongue influencing the performance and pressure pulsations of pump as turbine. ASME J. Fluids Eng. 136, 054501.

Yao, Z., Wang, F., Qu, L., Xiao, R., He, C., Wang, M., 2011. Experimental investigation of time-frequency characteristics of pressure fluctuations in a double-suction centrifugal pump. ASME J. Fluids Eng. 133, 101303.

Yun, L., Rongsheng, Z., Dezhong, W., Junlian, Y., Tianbin, L., 2016. Numerical and experimental investigation on the diffuser optimization of a reactor coolant pump with orthogonal test approach. J. Mech. Sci. Technol. 30, 4941–4948.

Zhang, N., Yang, M., Gao, B., Li, Z., Ni, D., 2015. Experimental investigation on unsteady pressure pulsation in a centrifugal pump with special slope volute. ASME J. Fluids Eng. 137, 061103.